

Novel Aperture-Coupled Microstrip-Line Feed for Circularly Polarized Patch Antenna

Hau Wah Lai*, Ka Ming Mak, and Ka Fai Chan

Abstract—A wideband circularly polarized patch antenna is proposed. The wide impedance and axial ratio bandwidths are achieved by the proposed feeding mechanism, which entails the use of a circular microstrip line coupling through four Γ -shaped slots to generate four sequentially phased sources to excite the single layer patch antenna. The proposed antenna can provide an SWR bandwidth of over 16.5% (for SWR < 1.5) and an axial-ratio bandwidth of 13.3% (for AR < 3 dB). The performance of the antenna has been confirmed by both measurement and simulation. The antenna gain is enhanced and backlobe radiation is reduced by placing a reflector at an optimized location.

1. INTRODUCTION

Circularly polarized (CP) antenna plays a major role in many wireless applications, such as RFID systems, and satellite communication and navigation systems. Nowadays, several global and regional satellite navigation systems such as the GPS, GLONASS and BEIDOU, etc., are in operation. It is desirable to have wideband antennas to account for manufacturing tolerance and accommodate two or more systems. There are many CP antenna designs available in the literature with very good performance, such as helix antenna, conical log spiral antenna or skew-planar wheel antenna. However, one of their major limitations is their bulky size, especially for portable wireless devices. Microstrip antennas are suitable and favorable for such application due to their low profile and light weight features. CP patch antenna can simply be illustrated by a square patch with truncated corners [1–3]. Other commonly known techniques are adding tails [2–4] or cutting slots [4–8] on the patches. It is also possible to use a U-shape feed line to feed a microstrip ring antenna [9]. Even though the above designs have CP characteristic, they exhibit an axial ratio bandwidth of less than 4%, which is not sufficient to accommodate for multiple navigation systems at the same time. To widen the axial ratio bandwidth, techniques like wideband feeding mechanism [10–12] and sequentially phased feeding networks [13–17] can be employed. The axial ratio bandwidths of CP patch antenna can be highly increased to over 10%. However, the geometries of the above wideband feeding mechanisms are complicated; while the sequentially phased feeding networks enlarge the size of the printed circuit or the ground plane.

In this paper, a new feeding mechanism for patch antenna with circular polarization is proposed. The antenna has a simple feeding geometry, which is an integration of a hook shape feed line and four Γ -slots only. The antenna has an impedance bandwidth of 16.5% (for SWR < 1.5), an axial ratio bandwidth of 13.5% (for AR < 3) and an average gain of 6 dB_{ic} across its operating frequency band. The antenna is very low profile, only $0.084\lambda_0$. Parametric studies of each portion of the antenna are provided. Gain enhancement and backlobe radiation suppression by placing a reflector at an optimized position are shown in the last section of the paper. Results show that a front-to-back ratio of 20 dB can be ensured within the operating bandwidth.

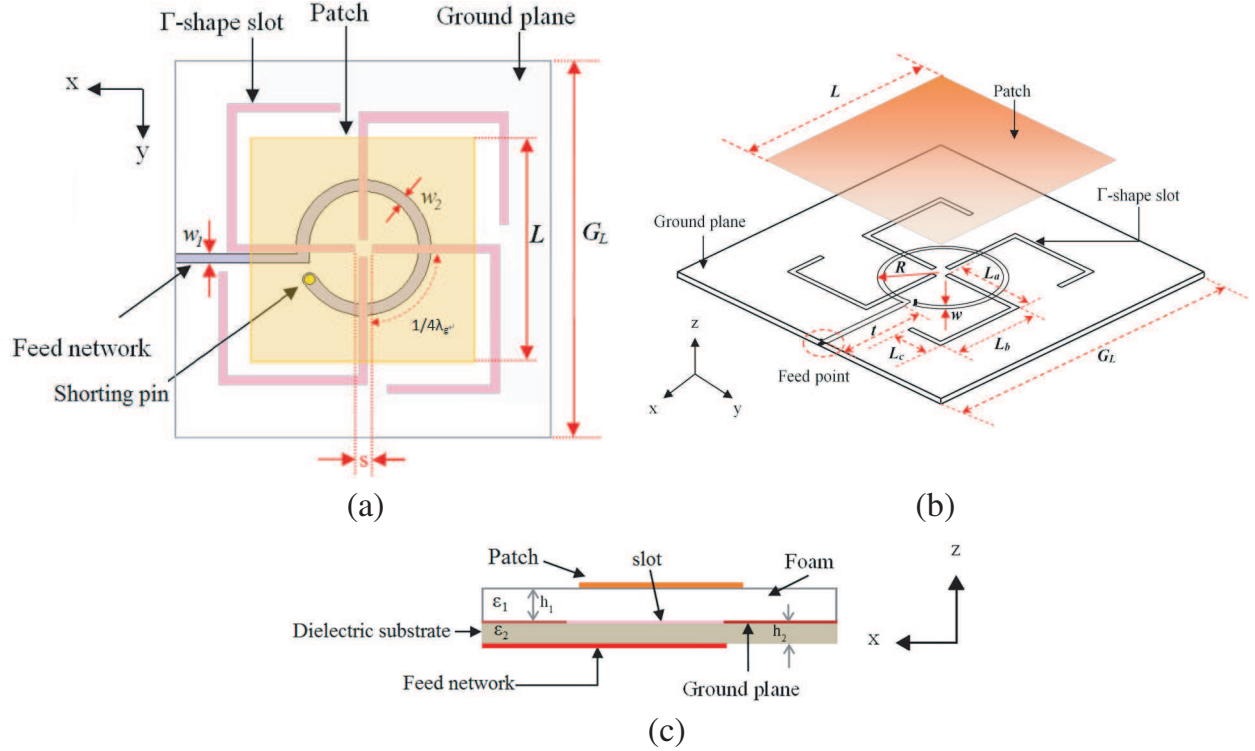
Received 18 October 2013, Accepted 28 November 2013, Scheduled 11 December 2013

* Corresponding author: Hau Wah Lai (hwterry@gmail.com).

The authors are with the State Key Laboratory of Millimeter Waves, City University of Hong Kong, Tat Chee Ave., Kowloon, Hong Kong, China.

2. ANTENNA GEOMETRY

The geometry of the proposed circularly polarized patch antenna is shown in Fig. 1. The antenna has two main portions, a metal patch at the top and a double sided printed-circuit-board (PCB) at the bottom and both of them are square. The bottom side of the double sided PCB has a microstrip line; while the top side of the double sided PCB has four Γ -shaped slots etched on the ground plane. It is noted that the centers of the metal patch and the double sided PCB are aligned together but they are located at different level along the z -direction. They are separated by a foam supporting block with a thickness of h_1 , which is 11 mm. The square patch has a length (L) of 43.4 mm and a thickness of 0.3 mm. The PCB has a thickness (h_2) of 1 mm, length (G_L) of 60 mm and dielectric constant $\epsilon_2 = 2.65$. The ground plane has four identical Γ -shaped slots with their orientation sequentially rotated about the center of the antenna by 0° , 90° , 180° and 270° respectively. The slot has a width of 1 mm and total length ($L_a + L_b + L_c = 20 \text{ mm} + 23.4 \text{ mm} + 17.5 \text{ mm}$) of 60.9 mm, which is around half a free-space wavelength at the center frequency. The separation between the opposite slots(s) is 3 mm. On the other side of the PCB is a hook shaped microstrip feed line. The radius of the ring is 10.75 mm. Its total length is around 70 mm, which is nearly one guided wavelength at the center frequency. The width of the feed line in the ring is w_2 (1.85 mm) and its line impedance is 63.5Ω . The open end of this ring shaped section is short-circuited to the ground plane. The length of the straight portion of the feed line is $1/4\lambda_g$ at the center frequency and its width is w_1 (1.15 mm) with a characteristic impedance of 82Ω . The impedances of the two sections of the feed line are obtained by optimization of the impedance and axial ratio bandwidths. The open end of the hook shaped feed line is connected to a 50Ω SMA connector.



	L	G_L	h_1	h_2	s	L_a	L_b	L_c	R	w_1	w_2	t
mm	43.4	60	11	1	3	20	23.4	17.5	10.75	1.15	1.85	21.1
λ_0	0.35	0.49	0.09	0.082	0.0245	0.16	0.19	0.14				0.17
λ_g						0.27	0.31	0.23	0.145	0.0155	0.025	0.28

Figure 1. Geometry of the proposed antenna. (a) Top view. (b) Perspective view. (c) Side view.

3. RESULTS

All the simulations of the proposed antenna are performed by using a commercial EM software HFSS (version 12). An optimized prototype was fabricated and tested. The SWR of the antenna was measured by an Agilent E5071C Network Analyzer, while the gain, axial ratio and radiation pattern of the antenna were measured by a SatimoStarLab system. Fig. 2 shows the simulated and measured SWRs of the proposed antenna. The results in Fig. 2 show that the antenna exhibits a measured impedance bandwidth of 16.5%, which is from 2.31 to 2.725 GHz (SWR < 1.5) while the simulated impedance bandwidth is 19.1% from 2.23 to 2.7 GHz. Fig. 3 shows the comparison of the measured and simulated axial ratios and gains of the proposed antenna versus frequency in the boresight direction. It is found that the measured 3 dB axial ratio bandwidth is about 13.3%, which is from 2.31 to 2.64 GHz, while the correspondence bandwidth by simulation is about 12.3%, which is from 2.322 to 2.627 GHz. The measured gain in the boresight direction has a peak gain of 7.37 dBi at 2.6 GHz and a gain around 6.5 dB_{ic} within the frequency range. The corresponding results by simulation are 5.8 dB_{ic} at 2.52 GHz and around 5 dB_{ic}.

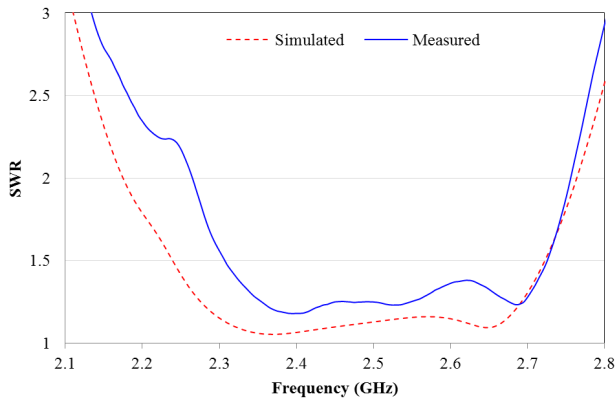


Figure 2. Simulated and measured SWR of the proposed antenna.

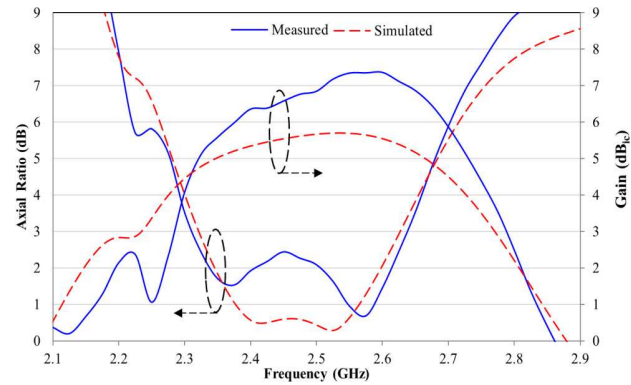


Figure 3. Axial ratio and gain against frequency of the proposed antenna.

Figure 3 also shows that the measured axial ratio curve has two local minimum points within the 3 dB axial ratio bandwidth, which are 2.37 GHz and 2.57 GHz respectively. The measured and simulated radiation patterns in $\phi = 0^\circ$ and $\phi = 90^\circ$ planes at these two frequencies are plotted in Fig. 4. At 2.37 GHz, it is seen that the difference between RHCP and LHCP by measurement and simulation are 15 dB and 20 dB, respectively, within the half-power beamwidth of the radiation pattern, and are 20 dB and 22 dB, respectively, in the boresight direction. The antenna has a 3 dB beamwidth of about 77° at $\phi = 0^\circ$ plane and about 71° at $\phi = 90^\circ$ plane by measurement. The correspondence simulated results are 76° and 74° , respectively, and the measured result is different from the simulated result only by less than 4%. The front-to-back ratio of the antenna at this frequency is about 6 dB by measurement and 5 dB by simulation.

At the second local minimum of the axial ratio curve at 2.57 GHz, the measured RHCP radiation is less than the LHCP radiation by 25 dB in the boresight direction. The radiation patterns of the RHCP by simulation and experiment are almost the same at $\phi = 0^\circ$ and $\phi = 90^\circ$ plane. The antenna has a measured 3 dB beamwidth of about 72° at $\phi = 0^\circ$ plane and about 69° at $\phi = 90^\circ$ plane with the simulated beamwidth results of 71° and 69° , respectively. The percentage difference between measurement and simulation is below 4%, which is the same as the result obtained at the 2.37 GHz. Both of the measured and simulated front-to-back ratios of the antenna at this frequency are about 5 dB.

4. PARAMETRIC STUDIES

In this section, a parametric study is carried out. All the parameters in Fig. 1 are optimized values using genetic algorithm. In optimization, we developed a custom-make genetic algorithm (GA) program,

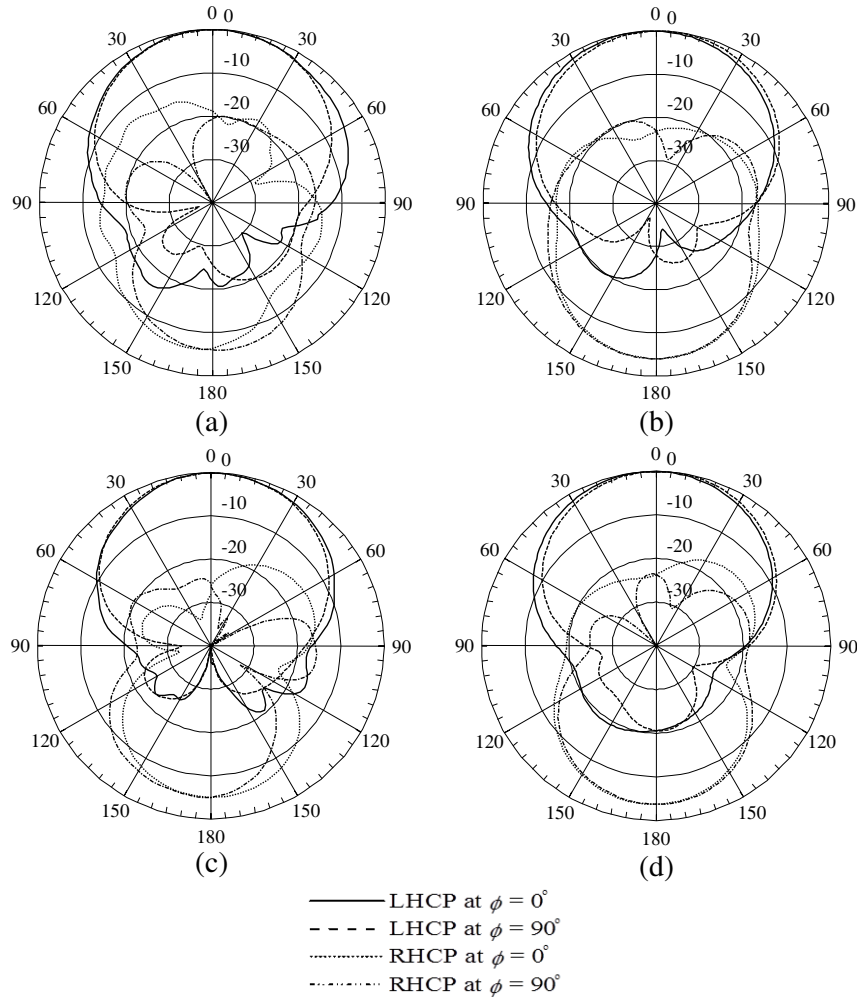


Figure 4. Measured and simulated and patterns in $\phi = 0$ and $\phi = 90$ planes of the proposed antenna. (a) 2.37 GHz by measurement. (b) 2.37 GHz by simulation. (c) 2.57 GHz by measurement. (d) 2.57 GHz by simulation.

which is linked with a simulator. Firstly, we need to set some requirements to the program; for example, the axial ratio and SWR of the antenna should be below 3 and 2 within a frequency range. Secondly, the program will start to simulate the performance of the antenna. When simulation is finished, the program will check if the results fulfill the requirements or not. If no, the program will automatically adjust the dimension of the antenna and simulate again; if yes, GA program will stop running, as an optimized parameters are found. With a given dielectric substrate for the microstrip feed line, we have only considered the effects of the patch height, patch length, slot length and slot separation on the antenna bandwidth. To simplify the study, only air substrate for the patch is used for all cases in this section. It is found that the SWR of the antenna is stable for all cases in this section. In contrast, the axial ratio of the antenna is relatively sensitive to the change of the above parameters. Therefore, only the results of axial ratio against frequency are presented in this section.

4.1. Patch Height

Patch antenna with a thicker substrate normally has a wider impedance bandwidth. However, there is an optimized patch height for the axial ratio bandwidth. Fig. 5 shows the simulated axial ratio for patch height of 9 mm, 10 mm, 11 mm and 12 mm. Other than the patch height, all the other parameters of the antenna are the same as the one in Fig. 1. It is found that the optimized patch height for having

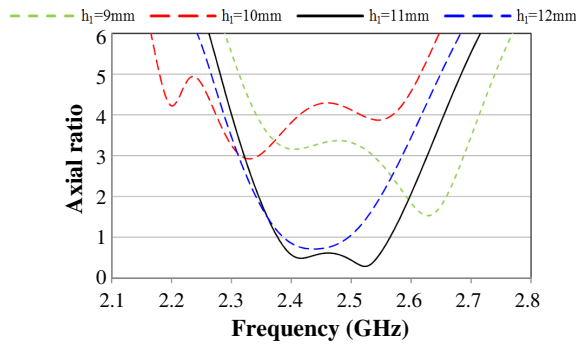


Figure 5. Simulated axial ratio against frequency for different values of h_1 .

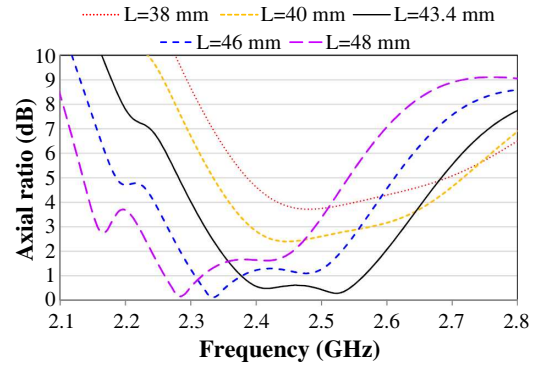


Figure 6. Simulated axial ratio against frequency for different values of L .

the widest axial ratio bandwidth is $h_1 = 11$ mm, which is around $0.09\lambda_g$. It is seen that the performance of the axial ratio bandwidth is relatively sensitive to the change of h_1 , especially when the substrate thickness is 10 mm. Therefore, choosing the right patch height is important.

4.2. Patch Length

Figure 6 shows the simulated results of the square patch with edge lengths of 38 mm, 40 mm, 43.4 mm, 46 mm and 48 mm. When the patch has a longer length, the center frequency of the axial ratio becomes lower and vice versa. This is in good agreement with the operating principle of patch antenna: the patch length is about half wavelength at the center frequency of the antenna. For $L = 43.4$ mm, 46 mm and 48 mm, similar percentage bandwidths are obtained for the axial ratio. This implies that the tolerance of the patch length is around ± 3 mm, and is around $\pm 7\%$, as well as the axial ratio bandwidth is not sensitive to the patch length.

4.3. Slot Length

The length of the Γ -shaped slot is highly related to the coupling from the feed line to the radiating patch. Fig. 7 shows the simulated results of the proposed antenna with different lengths of L_c . It is noted that the center frequencies of the antennas are relatively insensitive to the slot length but widest axial ratio bandwidth is achieved with the optimized value for $L_c = 17.5$ mm.

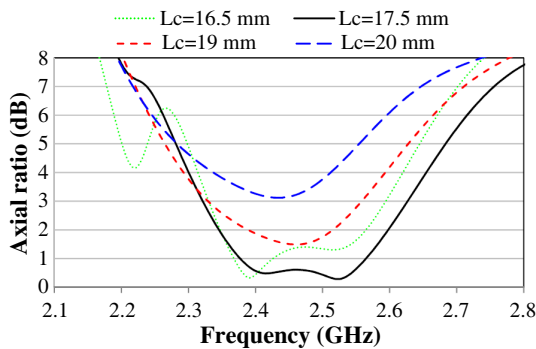


Figure 7. Simulated axial ratio against frequency for different values of slot length.

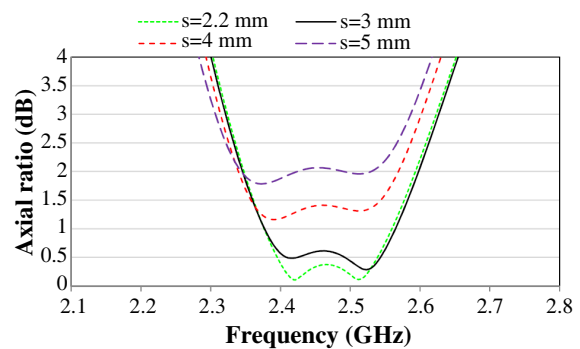


Figure 8. Simulated axial ratio against frequency for different values of slot separation.

4.4. Slot Separation

Figure 8 shows the simulated results of the proposed antenna with the slot separations of 2.2 mm, 3 mm, 4 mm and 5 mm. It is found that this separation can control the deepness of the axial ratio, while the coverage of the frequency range can be keeping almost the same. Therefore, this portion can be used to fine tune the axial ratio deepness of the proposed antenna.

5. DISCUSSION

5.1. Wideband Characteristic

Patch antenna in circular polarization can be fed by aperture coupling with a cross slot [6], and an axial ratio bandwidth of 2.5% can be obtained. However, this axial ratio bandwidth is too narrow and is necessary to be further enhanced. A single feeding cross-aperture coupled microstrip antenna with a hybrid matching is proposed in [18]. This CP antenna has the advantage of simple in structure and will not enlarge the antenna size. The axial ratio bandwidth of this antenna is enhanced to 4.6%. Even though the improvement is around 84% if compared with the design in [6], the axial ratio bandwidth of this antenna is still not wide enough for multiband applications, which need an axial ratio bandwidth up to 10%. The proposed antenna in this paper is similar to the antenna design in [18]. Both designs have a hybrid feeding network using aperture coupling. However, the proposed design has four Γ -shaped slots,

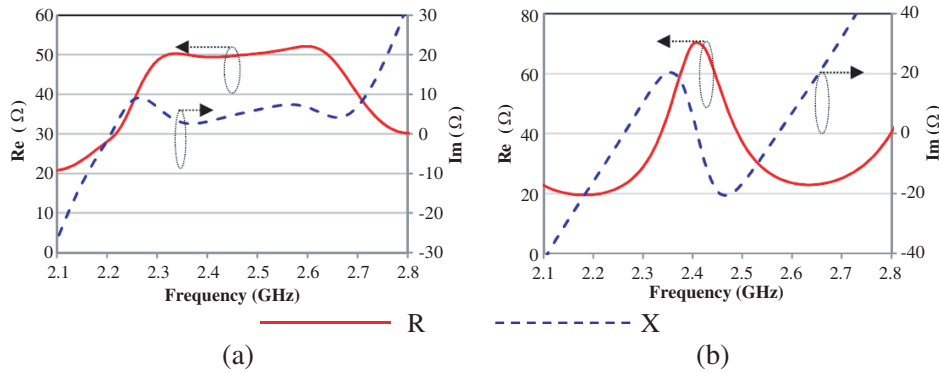


Figure 9. Simulated input impedance of the proposed antenna. (a) With patch. (b) Without patch.

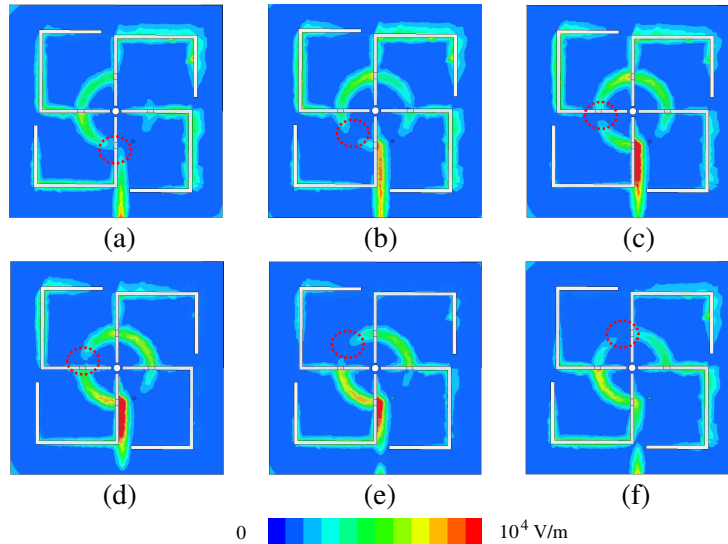


Figure 10. Current distribution of the feed line and ground plane of the proposed antenna for different values of the phase angle. (a) 0° . (b) 30° . (c) 60° . (d) 90° . (e) 120° . (f) 150° .

while the antenna design in [18] employed a cross-slot. The difference of the coupling slot results in a significant improvement in the impedance and axial ratio bandwidths by 65% and 190%, respectively, when compared to the cross slot design.

Figure 9(a) shows the input impedance of the proposed antenna. It can be seen that the input resistance curve has two peaks, which are at 2.35 GHz and 2.6 GHz. This implies that the antenna has two resonant modes. For these two modes, one mode is a patch mode, which operates at the same mode as the antenna in [18], and the other mode is a slot antenna mode, which is excited by the four Γ -shaped slots. Fig. 9(b) shows the input impedance when the patch of the proposed antenna is removed. It can be seen that there is only one resonant mode existing at 2.4 GHz when the patch is absent. The remaining resonant mode is very close to the lower resonant mode of the proposed antenna at 2.35 GHz. Since the patch is removed, it is strongly believed that this mode is the slot mode. On the other hand, this implies that the resonant mode at higher frequency is the patch mode.

Figure 10 shows the current distribution on the ground plane and the hook shape feed line of the proposed antenna for different values of phase angle. There is a red circle showing the minimum current of on the hook shape feed. It is observed that the current flows in a clockwise direction, which will contribute to a left-hand circular polarization.

5.2. Back Radiation Reduction

One of the simplest and most effective methods to reduce back radiation of an antenna is the use of a reflector at the back of the antenna, as shown in Fig. 11. There are two critical parameters to be optimized, namely, the length of the square reflector (R_L) and the separation between the antenna and reflector (R_S). Theoretically, the best position for putting a reflector is at a separation of $1/4\lambda_0$ behind the antenna and the size of the reflector is as large as possible. However, this is not practical in real application, which is due to size limitation of a device. Therefore, it is necessary to set a targeted front-to-back ratio and find out the smallest R_L and R_S for each optimization. In this paper, the targeted front-to-back ratio is 20 dB within the 3 dB axial ratio bandwidth. It is found that the optimized values of R_L and R_S are 80 mm ($\sim 0.66\lambda_0$) and 25 mm ($\sim 0.2\lambda_0$), respectively. Fig. 12 shows the gain at the front $[(\theta, \Phi) = (0^\circ, 0^\circ)]$ and the back $[(\theta, \Phi) = (180^\circ, 0^\circ)]$ of the proposed antenna with the optimized reflector. It is clearly showed that the low backlobe characteristic is achieved with reflector. Fig. 13

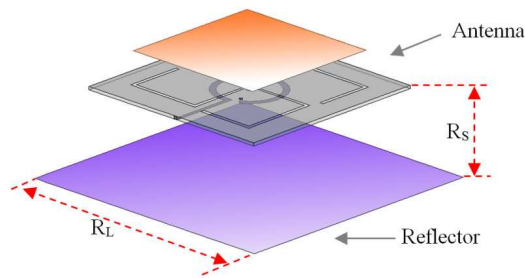


Figure 11. Geometry of the antenna with reflector.

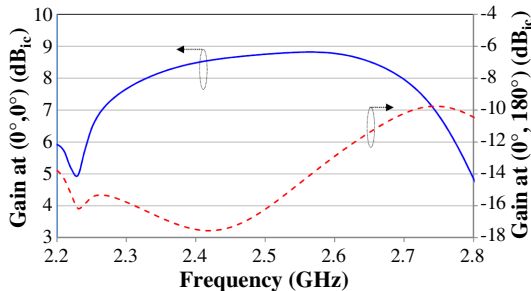


Figure 12. Gain against frequency of the proposed antenna with reflector.

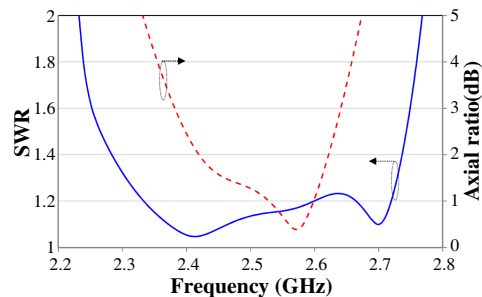


Figure 13. SWR and axial ratio against frequency of the proposed antenna with reflector.

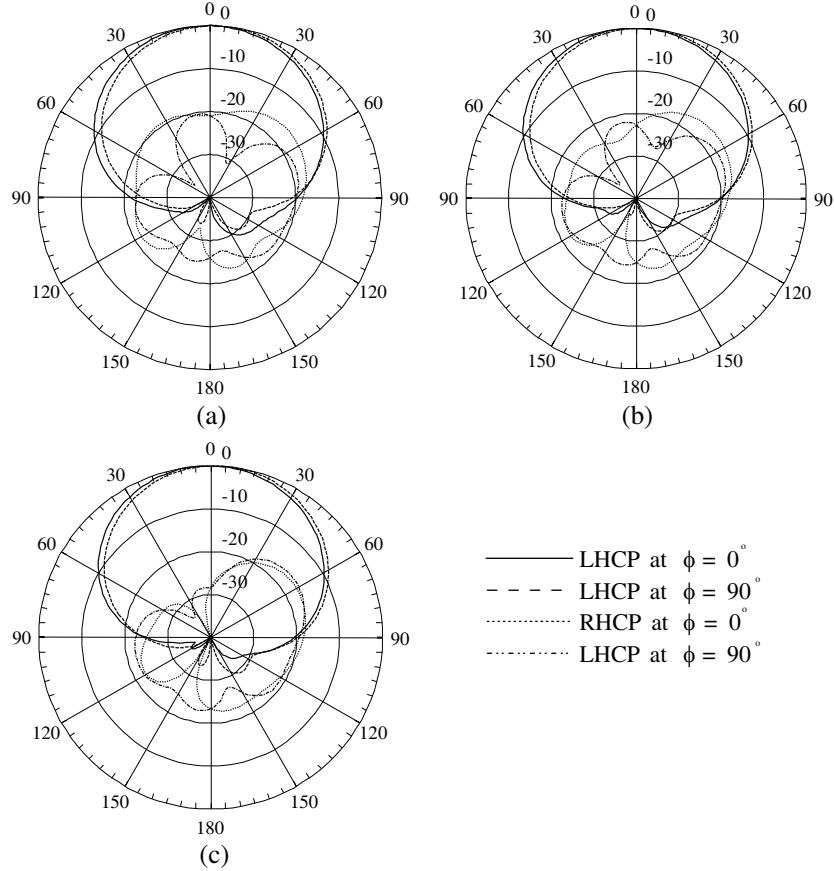


Figure 14. Radiation patterns with reflector. (a) 2.45 GHz. (b) 2.5 GHz. (c) 2.55 GHz.

shows the SWR and axial ratio of the corresponding antenna. It is observed that the wide impedance and axial ratio bandwidth characteristics remain unchanged, which are 21% and 10.5% respectively. The reflector can also increase the gain of the antenna. The simulated average gain of the antenna across its operating bandwidth is increased from about 5.5 dB_{ic} to about 8.5 dB_{ic} , which is a 3 dB enhancement.

The simulated radiation patterns of the antenna with the reflector at 2.45 GHz, 2.5 GHz and 2.55 GHz are shown in Fig. 14. It is observed that the radiation patterns are very stable and the back radiations are below -20 dB for all angles. The cross polarization levels at boresight and within the 3 dB beamwidth are below -16 dB across the operating bandwidth. Results show that adding a reflector is simple and effective for suppressing back radiation. The proposed antenna is suitable for wireless communications using circular polarization.

6. CONCLUSION

A new, simple and low cost single-feed method for circularly polarized microstrip patch antennas has been presented. The feeding geometry is based on aperture coupling technique using a hybrid feed line in hook shape and four Γ -shaped slots. The proposed antenna has wide impedance bandwidth, stable radiation pattern and wide axial ratio bandwidth. The measured SWR (< 1.5) and 3 dB axial ratio bandwidth of the antenna are over 16.5% and 13.3%, respectively. The peak gain of the antenna is 7.4 dB_{ic} at 2.55 GHz by measurement. The cross-polarization level is below 15 dB within the 3 dB beamwidth across the operating bandwidth. Simulations reveal the coupling mechanism of the hook shaped feed line and the four Γ -shaped slots. Adding a reflector at the optimized position can effectively enhance the front-to-back ratio up to 20 dB while the wideband characteristic of the antenna remains unchanged. Results show that the proposed antenna is suitable for nowadays wireless communication with circular polarization.

ACKNOWLEDGMENT

This work was supported by the Fundamental Research Program of Shenzhen City (No. JCYJ20120618140206431).

REFERENCES

1. Sharma, P. C. and K. C. Gupta, "Analysis and optimized design of single feed circularly polarized microstrip antennas," *IEEE Trans. on Antennas and Propagat.*, Vol. 31, No. 6, 949–955, Nov. 1983.
2. Yang, K. P. and K. L. Wong, "Dual-band circularly-polarized square microstrip," *IEEE Trans. on Antennas and Propagat.*, Vol. 49, No. 3, 377–382, Mar. 2001.
3. Chen, W. S., C. K. Wu, and K. L. Wong, "Compact circularly polarized microstrip antenna with bent slots," *Electron. Lett.*, Vol. 34, No. 13, 1278–1279, Jun. 1998.
4. Wong, H., K. K. So, K. B. Ng, K. M. Luk, C. H. Chan, and Q. Xue, "Virtually shorted patch antenna for circular polarization," *IEEE Antennas and Wireless Propagat. Lett.*, Vol. 9, 1213–1216, 2010.
5. Aksun, M. I., S. L. Chuang, and Y. T. Lo, "Theory and experiment of electromagnetically excited microstrip antennas for circular polarization operation," *IEEE Symposium on Antennas and Propagation digest*, Vol. 2, 1142–1145, San Jose, CA, USA, Jun. 1989.
6. Vlasits, T., E. Korolkiewicz, A. Sambell, and B. Robinson, "Performance of a cross-aperture coupled single feed circularly polarized patch antenna," *Electron. Lett.*, Vol. 32, No. 7, 612–613, Mar. 1996.
7. Huang, C. Y., J. Y. Wu, and K. L. Wong, "Cross-slot-coupled microstrip antenna and dielectric resonator antenna for circular polarization," *IEEE Trans. on Antennas and Propagat.*, Vol. 47, No. 4, 605–609, Apr. 1999.
8. Targonski, S. D. and D. M. Pozar, "Design of wideband circularly polarized aperture-coupled microstrip antennas," *IEEE Trans. on Antennas and Propagat.*, Vol. 41, No. 2, 214–220, Feb. 1993.
9. Tong, K. F. and J. Huang, "New proximity coupled feeding method for reconfigurable circularly polarized microstrip ring antennas," *IEEE Trans. on Antennas and Propagat.*, Vol. 56, No. 7, 1860–1866, Jul. 2008.
10. Nasimuddin, X. Qing, and Z. N. Chen, "Compact asymmetric-slit microstrip antennas for circular polarization," *IEEE Trans. on Antennas and Propagat.*, Vol. 59, No. 1, 285–288, Jan. 2011.
11. Tang, X. H., Y. L. Long, H. Wong, and K. L. Lau, "Broadband circularly-polarised patch antenna with 3D meandering strip feed," *Electron. Lett.*, Vol. 47, No. 19, 1060–1062, Sep. 2011.
12. Adrian, A. and D. H. Schaubert, "Dual aperture-coupled microstrip antenna for dual or circular polarization," *Electron. Lett.*, Vol. 23, No. 23, 1226–1228, Nov. 1987.
13. Bian, L., Y. X. Guo, L. C. Ong, and X. Q. Shi, "Wideband circularly-polarized patch antenna," *IEEE Trans. on Antennas and Propagat.*, Vol. 54, No. 9, 2682–2686, Sep. 2006.
14. Herscovici, N., Z. Sipus, and D. Bonafacic, "Circularly polarized single-fed wideband microstrip patch," *IEEE Trans. on Antennas and Propagat.*, Vol. 51, No. 6, 1277–1280, Jun. 2003.
15. Boccia, L., G. Amendola, and G. Di Massa, "Performance evaluation of shorted annular patch antennas for high-precision GPS systems," *IET Microw. Antennas Propagat.*, Vol. 1, No. 2, 465–471, 2007.
16. Guo, Y. X., K. W. Khoo, and L. C. Ong, "Wideband circularly polarized patch antenna using broadband baluns," *IEEE Trans. on Antennas and Propagat.*, Vol. 56, No. 2, 319–326, Feb. 2008.
17. Guo, Y. X., L. Bian, and X. Q. Shi, "Wideband circularly polarized annular-ring microstrip antenna," *IEEE Trans. on Antennas and Propagat.*, Vol. 57, No. 8, 2474–2477, Aug. 2009.
18. Kim, H., B. M. Lee, and Y. J. Yoon, "A single-feeding circularly polarized microstrip antenna with the effect of hybrid feeding," *IEEE Antennas and Wireless Propagat. Lett.*, Vol. 2, No. 1, 74–77, 2003.